Supplementary Materials and Methods

Sex-based differences in circulating microRNA and metabolite signatures associated with physical activity in Lynch Syndrome carriers

Contents

Contact information:
Minta Kärkkäinen: minta.e.m.karkkainen@jyu.fi
Tiina Jokela: tiina.a.jokela@jyu.fi (author of correspondence)

1. Supplementary Methods

1.1 Physical activity data

Daily physical activity was quantified as the metabolic equivalent of tasks per day (METd), combining leisure-time and commuting exercise, based on responses to four questions (Q1-4 listed below). In addition, self-reported physical activity level (SR-PA) was determined from a separate 7-point scale question (Q5).

METd values were missing for two participants and were imputed using the *mice* package in R. The imputation included relevant auxiliary variables: age, SR_PA, sex, body mass index (BMI), and a combined binary variable for previous cancer/upcoming cancer status. The study participants with either a previous cancer history or cancer that occurred after blood sampling were categorized as 1, and those with no previous or future cancer history were categorized as 0. Imputation was conducted using predictive mean matching (method = "pmm") with five imputed datasets (m = 5).

METd was calculated by summarizing equations 1 and 2:

Equation 1

$$\text{leisure time exercise MET} - \text{h/day} = \frac{(Q1 \times Q2 \times Q3) \div 60}{30}, \quad (1)$$

where Q1=leisure time exercise sessions per month; coding (1=0.5) (2=1.5) (3=4) (4=8) (5=15) (6=25), Q2=the strain of leisure time exercise; coding (1=4) (2=6) (3=10) (4=13), Q3=the duration of one exercise session; coding (1=7) (2=22) (3=45) (4=90) (5=150).

Equation 2

$$\text{commuting or school commuting exercise MET} - \text{h/day} = \frac{((Q4) \times 5 \times 4) \div 60}{7}, \quad (2)$$

where Q35=duration of commuting (including school trips); coding (1=0) (2=7) (3=22) (4=45) (5=75). 0 MET for participants who had not answered any of the questions but had indicated in the previous question that they don't exercise. Commuter exercise assumes walking = 4 MET.

Equation 3

$$\text{Total METd} = \text{Leisure time METh/day} + \text{Commuting METh/day} \quad (3)$$

7-scale self-reported physical activity question (SR-PA):

SR-PA was derived from a 7-scale question (Q5) on current activity level. Responses were recoded into three categories as follows: *Q5 coding**: (1–2 = low), (3–4 = intermediate), (5–7 = high)***

The questions used to scale physical activity level:

Q1. How many times per month do you currently engage in leisure-time physical activity?

☐ 1. Less than once a month

☐ 2. 1–2 times a month

☐ 3. 3–5 times a month

☐ 4. 6–10 times a month

☐ 5. 11–19 times a month

☐ 6. More than 20 times a month

Q2. The leisure-time physical activity you engage in is generally about as strenuous as:

☐ 1. Walking

☐ 2. Alternating walking and light jogging

☐ 3. Light jogging (jog)

☐ 4. Brisk running

Q3. On average, how long does one session of your leisure-time physical activity last?

☐ 1. Less than 15 minutes

☐ 2. 15 minutes – less than half an hour

☐ 3. Half an hour – less than one hour

☐ 4. One hour – less than two hours

☐ 5. Two hours or more

Q4. How much time do you spend daily commuting to work or school by walking, cycling, running, skiing, rollerblading, and/or other forms of active transportation?

☐ 1. Not at all

☐ 2. Less than 15 minutes

☐ 3. 15 minutes – less than half an hour

☐ 4. Half an hour – less than one hour

☐ 5. One hour or more

Q5. Which of the following descriptions best matches your current physical activity level?
(*select only one option*)

☐ 1. I do not exercise more than is necessary to manage daily activities

☐ 2. I do light walking and outdoor activities 1–2 times per week

☐ 3. I do light walking and outdoor activities several times per week

☐ 4. I do moderate exercise (e.g., yard work, walking, cycling) 1–2 times per week, which causes some shortness of breath and sweating

☐ 5. I do moderate exercise (e.g., yard work, walking, cycling) several times per week (3–5 times), which causes some shortness of breath and sweating

☐ 6. I do fitness training several times per week so that I sweat and breathe heavily during the activity

☐ 7. I participate in competitive sports and maintain my fitness through regular training

1.2 MicroRNA extraction

MicroRNA extractions from serum were done using the miRNeasy Serum/Plasma Advanced Kit (217204, Qiagen) by following the kit instructions. Briefly, the extraction of microRNAs was done using 0.5 mL of thawed serum. Samples were thawed on ice. The solutions needed for the isolation were provided in the kit and were added in amounts recommended by the manufacturer. To elute the isolated RNA, 20 µl of nuclease-free water was used and the samples were stored at -80˚C until library preparation.

1.3 MicroRNA library preparation

Small RNA library preparations were conducted using the QIAseq miRNA Library Preparation Kit (1103679, Qiagen) with multiplexing adapters, following the manufacturer's instructions. In summary, 5 µL of small RNAs were ligated to sequencing adapters at both the 5' and 3' ends, reverse transcribed into cDNA using UMI-assigning primers and purified with magnetic beads. A universal indexing sequence was incorporated during the reverse transcription step to differentiate samples during sequencing. Sample amplification was performed using a standard thermocycler (Eppendorf), after which it was purified, eluted into 15 µL of nuclease-free water, and stored at -20 °C until sequencing.

1.4. MicroRNA sequencing

The microRNA library sequencing was conducted on 5 separate analysis batches utilizing NextSeq 500 (Illumina) and NextSeq 500/550 High Output Kit v. 2.5 with 75 cycles (15057934, Illumina) to produce 75-base pair single-end reads with aimed mean sequencing depth of >5 M reads per sample as recommended by the manufacturer (Qiagen). The library sample concentrations were measured with a Qubit fluorometer (Invitrogen), quantified, diluted, and mixed into one pool in equal amounts (1.8-2 pM per sample) prior to sequencing.

1.5. MicroRNA alignment and filtering

Sequencing output data was obtained in FASTQ format using bcl2fastq software (v.2.20, Illumina, USA). FastQC was used for quality control. Before alignment, all four sample lanes (the sequencing produced 4 lanes for each sample) were merged to obtain the overall sample read count and to ensure better mapping quality. The QIAseq sequencing adapters were removed from the 3' end of the reads with FastX toolkit. Only sequences that contained the adapter and were at least 20 bp long after adapter removal were kept. After adapter clipping, the sequences were trimmed to maximum length of 22 bp to enrich microRNA-sequences and then quality filtered with FastX-toolkit. Only high-quality reads (Phred score >25) were selected for alignment to the reference genome. Subsequently, the pre-processed reads were mapped to human mature miRNA-genome (miRbase v.22) with Bowtie alignment tool. The mean raw read count of the experiments was 4,922,756 M reads for each sample, and after adapter removal, trimming, and filtering of low-quality data, the mean clean read count was 1,754,716 M counts per sample. On average, 1,163,087 M clean counts per sample were mapped to human miRNAs, achieving a mean alignment rate of 64 %. The remaining unmapped sequences represent clean read counts of other short RNAs, as the miRNeasy Serum/Plasma Advanced Kit extracts all short RNA molecules. The sequencing produced 1468 distinct microRNAs within the study cohort. The microRNA sequencing data generated in this study is available in NCBI Sequence Read Archive under bioproject PRJNA1275648. The microRNAs with low expression (<1 count per million in 50% of samples) were filtered, leaving 334 microRNAs for the main analyses. After normalization and accounting for the potential batch effect, the 334 microRNAs were used in the downstream analyses. The main manuscript describes the normalization procedure in the Materials and Methods section.

1.6. Metabolomics data

The metabolomics analyses were conducted on behalf of Nightingale Health Ltd. The serum samples were stored at -80 °C until analysis. Briefly, the metabolites were analyzed using a targeted proton nuclear magnetic resonance (1H-NMR) spectroscopy platform (Nightingale Health Ltd., Helsinki, Finland). The high-throughput 1H-NMR platform identifies small-molecule solutes from 300 µL of blood serum, such as distinct amino acids and glycolysis substrates, utilizing spectroscopic settings optimized to reduce interference from the broad spectral signals of lipoprotein particles. Additionally, the quantification of lipid constituents and the assessment of the spectrum of fatty acid saturation levels were performed using serum lipid extracts.

For the NMR measurements, 300 µL of serum and 300 µL of a sodium phosphate buffer (75 mM Na_2HPO_4 in 80%/20% H_2O/D_2O, pH 7.4; including also 0.08% sodium 3-(trimethylsilyl)propionate-2,2,3,3-d_4 and 0.04% sodium azide) are mixed and transferred to the NMR tubes. The liquid handling steps of the serum samples are conducted using a PerkinElmer JANUS Automated Workstation equipped with an 8-tip dispense arm with Varispan. Nightingale's NMR metabolomics analyses use the Bruker AVANCE III 500 MHz spectrometers with the SampleJet robotic sample changer. The 500 MHz spectrometer is equipped with a selective inverse room temperature probe head. Nightingale uses standardized parameters for data acquisition. After the measurements, the samples are handled with a standardized lipid extraction procedure containing multiple extraction steps including saturated sodium chloride solution, methanol, dichloromethane, and

deuterochloroform. The lipid extracts are transferred into the NMR tubes and the extracted lipid (LIPID) data are collected in full automation with the 600 MHz instrument using a standard parameter set. The initial data processing, including Fourier transformations of NMR spectra and automated phasing, is carried out by the computers controlling the spectrometers. The processed spectra are then automatically transferred to a centralized server, where additional automated steps take place, such as checking for missing or extra peaks, background control, baseline correction, and spectral alignment for specific regions. The spectral data of each sample is also compared against two quality control samples, with their data being tracked and assessed over time. Regression modeling is applied to spectral regions that pass all quality control checks to generate quantified molecular data. Additionally, individual metabolic measures undergo statistical quality control and are cross-checked against a comprehensive molecular database. Only the metabolic measures that successfully meet all quality criteria are stored and made available for epidemiological analyses. The in-detail technicalities of the method have been reported previously by Soininen et al. (https://pubs.rsc.org/en/content/articlelanding/2009/an/b910205a). A description of the NMR instrument models and the experimental workflow used by Nightingale Health can be found in this publication (including the supplementary material): https://pubmed.ncbi.nlm.nih.gov/36737450/.

1.7 Omics-level differences between self-reported physical activity groups

Principal Coordinates Analysis (PCoA), utilizing the base stats package in R, was used to explore and visualize circulating microRNA and circulating metabolite-level similarities or dissimilarities between SR-PA groups. The distance matrix was determined using Manhattan distances to assign a location for each study subject in low-dimensional space. The PCoA coordinates were visualized using a scatter plot. Permutational Analysis of Variance (PERMANOVA) was used to test whether the centroids and dispersion of the PCoA matrix differed between groups, while Analysis of Similarities (ANOSIM) was applied to assess whether within-group similarity exceeded that between groups. Both statistical tests were conducted using the *vegan* R package.

1.8 Circulating microRNA and metabolite co-expression module correlations with physical activity levels

Weighted Correlation Network Analysis (WGCNA), utilizing the R package WGCNA, was used to investigate how clustered circulating microRNAs and clustered circulating metabolites correlate with METd levels. A gene expression similarity matrix was first computed and transformed into an adjacency matrix using a soft-thresholding power of 7 for microRNAs, and 20 for metabolites (Supplementary Figure S1) to approximate scale-free topology. The adjacency matrix was then converted into a topological overlap matrix (TOM), capturing both direct and indirect gene interactions. Hierarchical clustering was applied to the TOM to identify modules with high co-expression. Each module was summarized by its eigengene (ME), defined as the first principal component of the expression or level profiles within that module. Relationships with METd were assessed using biweighted midcorrelation, with significance determined by p-values and FDR correction using the Benjamini-Hochberg (BH) procedure. Additionally, module-BMI and module-age correlations were calculated using biweighted midcorrelation and module-previous cancer history correlations using Pearson correlation. Heatmaps, scatter plots (with robust regression lines), and boxplots were used to visualize the key findings. The structural equation modeling (SEM), using the R lavaan package, was used to study whether METd, daily energy intake (kJ) or fat consumption (g/d) have indirect effects on module levels via BMI.

The circulating microRNAs and metabolites from WGCNA modules that exhibited the strongest correlations with METd were further analyzed. Biweighted midcorrelation analyses were performed separately between each PA-associated c-miRNAs or c-Metabs and METd values. The FDR was controlled using the BH procedure. Only microRNAs and metabolites with FDR <0.05 were selected for further analysis to examine their interrelationships.

1.9 Circulating microRNA gene enrichment and pathway analyses

To study whether physical activity-level-associated module microRNAs are overrepresented in cancer, we used miEAA's Over-representation analysis (ORA) -tool. The MNDR Diseases (subcategory cancer) with adj. p-value <0.05 were deemed over-represented in cancer. We also explored the potential biological roles of physical-activity-associated module microRNAs using miRWalk for target gene predictions, focusing on 3' UTR targets. Only genes confirmed by TargetScan, miRDB, and miRTarBase were retained for gene set enrichment analysis (GSEA). KEGG pathway enrichment was analyzed, with significance defined by BH adjusted p-values ≤ 0.05.

1.10 miRNATissueAtlas analysis to explore physical activity-associated circulating microRNA source tissues

Expression data (version 3) and associated metadata were downloaded from the miRNATissueAtlas 2025 database. Expression levels of selected miRNAs across various human tissues were visualized using strip plots. For each miRNA, expression values were log-transformed and plotted by tissue group, with sample sex indicated by color. Plots were generated using Python libraries matplotlib and seaborn.

1.11 Regularized canonical correlation analysis (rCCA)

Canonical correlation analysis (CCA), using R package miXOmics, was applied to evaluate the correlation structure between the two omics layers: circulating microRNAs and metabolites, which had significant correlations with METd. To reduce the dimensionality of the data and maximize the correlation between the two datasets, regularized CCA (rCCA) was performed using ridge regression as the regularization method. To explore potential sex-based differences in the relationships between microRNAs and metabolites, the data were split by sex. Separate analyses were performed for females and males by determining appropriate regulation parameters for both groups. The results of the rCCA were visualized using a clustered heatmap.

1.12 Acute exercise intervention, serum sample collection and RT-qPCR analysis

As acute exercise pout, 11 cancer-free LS carriers from Finland (8 females and 3 males) conducted a validated submaximal bicycle ergometer test (Beekley MD, et. al. (2004) (Cross-Validation of the YMCA Submaximal Cycle Ergometer Test to Predict VO2max) during February-June of 2025 (AgeCanLS project). The age range of the participants was 42-71. The study participant pedalled on the cycle ergometer for 3 minutes at a resistance of 0 kg and a cadence of 50-55 (this is the warm-up). As a first stage of the test, the participant pedalled for 3 minutes at 25 W, 50-55 cadence (150 kgm/min =0.5 kg). The heart rate was recorded at 2 minutes and 3 minutes. If the heart rate values were not within 5 bpm, cycling was continued for another minute and recorded at 4 minutes. Based on the steady-state heart rate (HR) reached, the workload was increased for the second stage based on the details listed in the Table below (note: 6 kgm/min = 1 Watt). The test included 4 stages, each lasting for 3 minutes. If the participant did not reach 85% of age-predicted HR, cycling continued to additional 5th stage. After the test phase, the theoretical maximum workload was calculated and cycling continued for 10 minutes at 50% of the theoretical maximum workload.

Workloads

	HR<80	**HR 80-89**	**HR90-100**	**HR>100**
2nd stage	125 W	100 W	75 W	50 W
3rd stage	150 W	125 W	100 W	75 W
4th stage	175 W	150 W	125 W	100 W
(5th stage)	200 W	175 W	150 W	125 W
10 min end cycling (50 % of theoretical max workload)				

The blood samples were collected at baseline (timepoint a), immediately after exercise (timepoint b) and 1h post-exercise (timepoint c). Venous blood samples from all participants were drawn from the antecubital vein using 9 ml KE2 K2EDTA tubes (455 045, Greiner Bio-One). Serum was separated from whole blood by allowing the samples to clot for 30 min at room temperature, followed by centrifugation at 1800 x g for 10 min. The samples were aliquoted and stored at -80°C until analysis. The small RNAs were extracted from serum samples following the same protocol described under the heading: 1.2 MicroRNA extraction, and stored at -80°C. The samples were reverse transcribed as cDNA using Qiagen's miRCURY LNA RT Kit (339340) according to the manufacturer's instructions. Briefly, the reverse transcription master mix was prepared on ice, and 7 µL of RNA sample was mixed with 3 µL of master mix by carefully pipetting. The samples were incubated for 60 min at 42°C following 5 min at 95°C to inactivate the Reverse Transcriptase Enzyme and immediately cooled to 4°C using a standard thermocycler (Eppendorf). The reverse transcription reactions were stored at -20°C until qPCR.

The qPCR was conducted using Qiagen's miRCURY LNA™ Green PCR Kit (339346). Briefly, a reaction mix for each miRCURY LNA miRNA PCR Assay primer (339306) (*hsa-miR-885-3p: YP00204136; hsa-miR-483-5p: YP00205693; hsa-miR-374a-5p: YP00204758; hsa-miR-301a-3p: YP00205601; and cel-miR-39-3p* spike-in control*: YP00203952*) was prepared on ice according to the manufacturer's instructions. 3 µL of cDNA 1:10 dilution was added to 7 µL of master mix and carefully

mixed by pipetting. The samples were incubated 2 min at 95 °C, followed by 40 cycles in conditions: 10 s at 95 °C and 60 s at 56 °C using Cielo Thermal Cycler or BioRad's C1000 Touch Thermal Cycler. Delta Cq values were calculated by Cq (reference) – Cq (target), where Cq(reference) was calculated as the average Cq of all miRNAs at baseline (Pre-exercise). Line plots were used to visualize the changes in miRNA expression over time.

1.13 R scripts

All R scripts used for computational analyses are publicly available at:
https://github.com/karkmiee/Lynch_syndrome_PA_omics/tree/main

1.14 Phenodata

By ethical standards and to protect the privacy of study participants, the phenotypic data (e.g., age, BMI, physical activity data, cancer history, and related information) used in the statistical analyses cannot be made publicly available. The data supporting the findings of this study are available from the corresponding author upon request.

1.15 Additional files

Large supplementary Excel tables are provided in a separate file titled *Additional_tables.xlsx*. Other supplementary tables, along with Supplementary Figures, are included in this *Supplementary Materials & Methods* file under the sections titled *Supplementary Tables* and *Supplementary Figures*.

2. Supplementary Tables

Supplementary Table 1. Sequencing coverage and quality statistics of each sample. MicroRNAs were mapped to human mature miRNA-genome (miRbase v.22). On average, 1,163,087 M clean counts per sample were mapped to human miRNAs, achieving a mean alignment rate of 64 %. The remaining unmapped sequences represent clean read counts of other short RNAs, as the miRNeasy Serum/Plasma Advanced Kit extracts all short RNA molecules. The sequencing produced 1468 distinct microRNAs within the study cohort.

Sample ID	Total number of sequenced reads	Total number of clean sequenced reads	Total number of uniquely mapped microRNA aligned sequence reads	MicroRNA alignment %	NGS experiment number
1	3740680	2657405	1727579	65,0	1
2	3639260	2213072	1194616	54,0	1
3	4261298	2682312	1551717	57,9	1
4	2222496	850701	226457	26,6	1
5	4871359	1147725	697587	60,8	3
6	2502302	1565709	1026949	65,6	1
7	1585020	845814	553670	65,5	2
8	9129525	3059302	2180388	71,27	5
9	4913957	263584	148240	56,2	2
10	5109876	1247341	835469	67,0	2
11	8154146	909515	476959	52,44	5
12	4071039	1122018	760504	67,8	2
13	3879327	188662	760504	67,8	2
14	3714238	1272472	835251	65,6	3
15	8955546	3838576	3153755	82,16	5
16	3144129	1173055	758497	64,7	3
17	2434188	1578987	828652	52,5	1
18	3022779	1922110	1163069	60,5	1
19	1557905	977090	558798	57,2	1
20	5124394	2107865	1297391	61,6	2
21	7449211	2903457	1407104	48,46	5
22	1023146	334823	264778	79,1	3
23	2256265	927431	300580	32,4	1
24	4126351	1624267	1104502	68,0	1
25	4491075	2188813	1088278	49,7	1

26	3806260	2609133	2233157	85,6	1
27	2212775	948741	243067	25,6	1
28	2595748	878742	463624	52,8	1
29	2758630	1095736	666755	60,9	1
30	7907793	263100	137028	52,08	5
31	6335293	2355244	1310220	55,6	4
32	6045407	867915	421479	48,56	5
33	8147271	993739	587884	59,16	5
34	9127129	1266413	706114	55,76	5
35	2407378	1497518	1056798	70,6	1
36	3077048	1399924	908131	64,9	1
37	8557830	2135882	1395795	65,35	5
38	3560635	2222714	1488774	67,0	1
39	8418266	1529053	1014130	66,32	5
40	5025407	2326499	1566897	67,4	3
41	8578539	2635314	1911714	72,54	5
42	5339248	4316894	4065651	94,2	3
43	3501497	2326197	1581116	68,0	1
44	3484467	1898310	1124369	59,2	3
45	8987063	1807260	1074253	59,44	5
46	3088668	1859142	947233	51,0	1
47	3580227	2096321	1204127	57,4	1
48	3555370	2286197	599898	26,2	1
49	5538671	1871225	1256570	67,2	4
50	5243371	1801072	1432711	79,5	4
51	3255616	1636776	1231183	75,2	3
52	3821925	2691913	1839653	68,3	1
53	8962420	4394109	3066995	69,80	5
54	5544303	532069	405703	76,3	2
55	2246559	1244461	497038	39,9	1
56	8384410	2249250	1049961	46,68	5
57	7918159	1916372	1010257	52,72	5
58	6362125	1427147	701803	49,2	4
59	4600904	2214827	1595027	72,0	4

60	6193974	524566	380831	72,6	4
61	4158660	1133085	905108	79,9	3
62	3498996	1279983	1011187	79,0	2
63	6498834	1959171	1629515	83,2	4
64	4348292	699138	537497	76,9	3
65	4208672	2144152	1572092	73,3	2
66	5564550	2002770	1216930	60,76	5
67	4154330	1685414	1349511	80,1	3
68	4921665	689803	605993	87,9	4
69	5718758	3014031	1782799	59,2	2
70	4117070	3066551	2275381	74,2	3
71	3295089	2022602	1248148	61,7	3
72	6035292	1683609	950202	56,4	4
73	6912564	1215811	862655	71,0	4
74	1988898	1178888	926252	78,6	2
75	8734894	3157102	2576965	81,6	4
76	2062633	1021260	584671	57,3	3
77	3985984	2178874	1756608	80,6	2
78	3296463	1679190	1201293	71,5	2
79	5531534	3456993	2484541	71,9	2
80	6707081	2307250	1744176	75,6	4
81	7858850	3300248	2205613	66,83	5
82	6014121	3602895	2643804	73,4	2
83	1289001	726877	462439	63,6	2
84	8734385	3009878	2092214	69,51	6
85	4246355	914245	646828	70,8	2
86	1475693	594181	125491	21,1	2
87	6318488	1869462	1021829	54,66	5
88	5766097	1469244	1224695	83,4	4
89	5653397	993885	821817	82,7	4
90	5633955	522207	347875	66,6	4
91	4663150	1278217	958155	75,0	4
92	4471752	1078397	833289	77,3	4
93	6400881	2531331	1484301	58,6	4

Supplementary Table 2. False discovery rate correction of module-METd correlation significance.

Module	Omics	Method	Adj.P-value		
			Full cohort	Female	Male
MEglaucous	c-miRNA	BH	0.22	0.71	0.91
MEgreen	c-miRNA	BH	0.22	0.71	0.46
MEblue	c-miRNA	BH	0.5	0.97	0.45
MEyellow	c-Metab	BH	0.003	0.007	0.56
MEturquoise	c-Metab	BH	0.017	0.007	0.56
MEpink	c-Metab	BH	0.003	0.003	0.56

Supplementary Table 3. Correlation of physical-activity-associated co-expression modules and BMI, age and previous cancer history. Biweighted midcorrelation was used to study the correlation between BMI, age and module, whereas Pearson correlation was used to study the correlation between previous cancer history and module expression level. Significant correlations are highlighted in yellow (p-value).

Module	Omics	Variable	Correlation (p-value)		
			Full cohort	Female	Male
MEglaucous	c-miRNA	BMI	-0.28	-0.35	-0.21
			(7.47e-03)	(0.014)	(0.175)
		Age	0.07	-0.01	0.20
			(0.516)	(0.932)	(0.191)
		Previous	0.15	0.16	0.13
		cancer	(0.159)	(0.270)	(0.4)
MEgreen	c-miRNA	BMI	0.32	0.32	0.26
			(0.002)	(0.024)	(0.089)
		Age	0.12	0.27	-0.08
			(0.258)	(0.058)	(0.592)
		Previous	0.11	0.22	-0.05
		cancer	(0.292)	(0.134)	(0.758)
MEblue	c-miRNA	BMI	-0.24	-0.25	-0.22
			(0.02)	(0.09)	(0.150)
		Age	-0.01	-0.22	0.19
			(0.942)	(0.137)	(0.219)
		Previous	-0.01	-0.22	0.2
		cancer	(0.942)	(0.121)	(0.191)
MEyellow	c-Metab	BMI	-0.491	-0.457	-0.599
			(5.76e-07)	(0.001)	(1.77e-05)
		Age	0.024	-0.03	0.210
			(0.818)	(0.837)	(0.170)
		Previous	0.09	0.07	0.1
		cancer	(0.409)	(0.638)	(0.515)
MEturquoise	c-Metab	BMI	0.405	0.354	0.473
			(5.57e-05)	(0.013)	(1.18e-03)
		Age	0.103	0.259	-0.113
			(0.327)	(0.072)	(0.464)
		Previous	-0.02	0.12	-0.22
		cancer	(0.815)	(0.410)	(0.154)
MEpink	c-Metab	BMI	-0.427	-0.375	-0.546
			(1.97e-05)	(0.008)	(1.28e-04)
		Age	-0.099	-0.143	-0.072
			(0.343)	(0.327)	(0.644)
		Previous	-0.03	-0.07	0.02
		cancer	(0.781)	(0.638)	(0.890)

Supplementary Table 4. Results of the structural equation model (SEM) examining associations between physical activity, diet, BMI, and circulating microRNA modules. The table summarizes the direct and indirect relationships among daily metabolic equivalent of tasks (METd), fat intake, energy intake, sex, body mass index (BMI), and circulating miRNA modules (MEglaucous, MEgreen, and MEblue). Reported values include unstandardized estimates, *p*-values, standardized coefficients (β), and an interpretation of each pathway. Direct effects refer to relationships between predictors and BMI. Indirect effects represent mediated pathways from METd through BMI to circulating miRNA modules. Significant and marginal associations are noted based on *p*-values.

Pathway	Estimate	p-value	Standardized β	Interpretation
Direct effects on BMI				
METd → BMI	-0.326	0.009	-0.264	Significant: higher physical activity → lower BMI
Fat intake → BMI	-0.038	0.470	-0.246	Not significant
Energy intake (kJ) → BMI	0.000	0.609	0.176	Not significant
Sex → BMI	0.582	0.626	0.051	Not significant
Indirect effects via BMI				
METd → BMI → MEglaugous	+0.001	0.085.	+0.062	Marginal, not significant
METd → BMI → MEgreen	-0.002	0.064.	-0.070	Marginal, not significant
METd→ BMI → MEblue	+0.001	0.095.	+0.060	Marginal, not significant
Total indirect effect (via BMI)	+0.001	0.353	+0.052	Overall not significant

Supplementary Table 5. Results of the structural equation model (SEM) examining associations between physical activity, diet, BMI, and circulating metabolite modules. The table summarizes the direct and indirect relationships among daily metabolic equivalent of tasks (METd), fat intake, energy intake, sex, body mass index (BMI), and circulating metabolite modules (MEyellow, MEturquoise, and MEpink). Reported values include unstandardized estimates, *p*-values, standardized coefficients (β), and an interpretation of each pathway. Direct effects refer to relationships between predictors and BMI. Indirect effects represent mediated pathways from METd through BMI to circulating metabolite modules. Significant and marginal associations are noted based on *p*-values.

Pathway	Estimate	p-value	Standardized β	Interpretation
Direct effects on BMI				
METd → BMI	-0.326	0.009	-0.264	Significant: higher physical activity → lower BMI
Fat intake → BMI	-0.038	0.470	-0.246	Not significant
Energy intake (kJ) → BMI	0.000	0.609	0.176	Not significant
Sex → BMI	0.582	0.626	0.051	Not significant
Indirect effects via BMI				
METd → BMI → MEyellow	0.002	0.025	0.102	Significant positive indirect effect
METd → BMI → MEturquoise	-0.002	0.044	-0.083	Significant negative indirect effect
METd → BMI → MEpink	0.002	0.034	0.095	Significant positive indirect effect
Total indirect effect (via BMI)	0.003	0.032	0.114	Overall significant mediation effect

Supplementary Table 6. Cancer over-representation analysis of physical activity-associated c-miRNAs.

Subcategory	Enrichment	P-value	P-adjusted	Observed	miRNAs/precursors
Module glaucous					
Kidney chromophobe cancer	over-represented	6.68e-5	0.0040615	6	hsa-miR-1307-5p; hsa-miR-26a-5p; hsa-miR-301a-3p; hsa-miR-374a-5p; hsa-miR-590-3p; hsa-miR-30d-3p
Module green					
Prostate cancer	over-represented	1.45e-8	6.76e-7	16	hsa-miR-122-5p; hsa-miR-125b-5p; hsa-miR-128-3p; hsa-miR-148a-3p; hsa-miR-152-3p; hsa-miR-192-5p; hsa-miR-193b-5p; hsa-miR-194-5p; hsa-miR-27b-3p; hsa-miR-28-3p; hsa-miR-30d-5p; hsa-miR-34a-5p; hsa-miR-378c; hsa-miR-483-5p; hsa-miR-95-3p; hsa-miR-885-3p
Progesterone-receptor negative breast cancer	over-represented	5.86e-8	1.78e-6	16	hsa-miR-122-5p; hsa-miR-125b-5p; hsa-miR-128-3p; hsa-miR-146b-3p; hsa-miR-148a-3p; hsa-miR-152-3p; hsa-miR-192-5p; hsa-miR-193a-5p; hsa-miR-193b-5p; hsa-miR-194-5p; hsa-miR-28-3p; hsa-miR-30d-5p; hsa-miR-34a-5p; hsa-miR-483-5p; hsa-miR-95-3p; hsa-miR-885-3p
Lung cancer	over-represented	1.38e-7	3.06e-6	16	hsa-miR-122-5p; hsa-miR-125b-5p; hsa-miR-128-3p; hsa-miR-146b-3p; hsa-miR-152-3p; hsa-miR-192-5p; hsa-miR-193a-5p; hsa-miR-193b-5p; hsa-miR-194-5p; hsa-miR-27b-3p; hsa-miR-28-3p; hsa-miR-30d-5p; hsa-miR-34a-5p; hsa-miR-483-5p; hsa-miR-95-3p; hsa-miR-885-3p
Estrogen-receptor positive breast cancer	over-represented	1.63e-7	3.24e-6	16	hsa-miR-122-5p; hsa-miR-125b-5p; hsa-miR-128-3p; hsa-miR-146b-3p; hsa-miR-148a-3p; hsa-miR-152-3p; hsa-miR-192-5p; hsa-miR-193a-5p; hsa-miR-193b-5p; hsa-miR-194-5p; hsa-miR-28-3p; hsa-miR-30d-5p; hsa-miR-34a-5p; hsa-miR-483-5p; hsa-miR-95-3p; hsa-miR-885-3p
Progesterone-receptor positive breast cancer	over-represented	1.59e-7	3.24e-6	16	hsa-miR-122-5p; hsa-miR-125b-5p; hsa-miR-128-3p; hsa-miR-146b-3p; hsa-miR-148a-3p; hsa-miR-152-3p; hsa-miR-192-5p; hsa-miR-193a-5p; hsa-miR-193b-5p; hsa-miR-194-5p; hsa-miR-27b-3p; hsa-miR-28-3p; hsa-miR-34a-5p; hsa-miR-483-5p; hsa-miR-95-3p; hsa-miR-885-3p
Breast cancer luminal	over-represented	1.90e-7	3.59e-6	11	hsa-miR-125b-5p; hsa-miR-128-3p; hsa-miR-148a-3p; hsa-miR-192-5p; hsa-miR-193a-5p; hsa-miR-193b-5p; hsa-miR-194-5p; hsa-miR-28-3p; hsa-miR-34a-5p; hsa-miR-483-5p; hsa-miR-95-3p
Estrogen-receptor negative breast cancer	over-represented	5.31e-7	8.23e-6	15	hsa-miR-122-5p; hsa-miR-125b-5p; hsa-miR-128-3p; hsa-miR-146b-3p; hsa-miR-152-3p; hsa-miR-192-5p; hsa-miR-193a-5p; hsa-miR-193b-5p; hsa-miR-194-5p; hsa-miR-27b-3p; hsa-miR-30d-5p; hsa-miR-34a-5p; hsa-miR-483-5p; hsa-miR-95-3p; hsa-miR-885-3p
Bladder cancer	over-represented	1.42e-6	1.68e-5	8	hsa-miR-125b-5p; hsa-miR-148a-3p; hsa-miR-152-3p; hsa-miR-192-5p; hsa-miR-193a-5p; hsa-miR-27b-3p; hsa-miR-28-3p; hsa-miR-34a-5p

Breast cancer	over-represented	3.43e-6	3.38e-5	17	hsa-miR-122-5p; hsa-miR-125b-5p; hsa-miR-128-3p; hsa-miR-146b-3p; hsa-miR-148a-3p; hsa-miR-152-3p; hsa-miR-192-5p; hsa-miR-193a-5p; hsa-miR-193b-5p; hsa-miR-194-5p; hsa-miR-27b-3p; hsa-miR-28-3p; hsa-miR-30d-5p; hsa-miR-34a-5p; hsa-miR-483-5p; hsa-miR-95-3p; hsa-miR-885-3p
Basal-like breast cancer	over-represented	3.59e-6	3.48e-5	9	hsa-miR-122-5p; hsa-miR-128-3p; hsa-miR-192-5p; hsa-miR-193a-5p; hsa-miR-193b-5p; hsa-miR-194-5p; hsa-miR-30d-5p; hsa-miR-34a-5p; hsa-miR-483-5p
Her2-receptor positive breast cancer	over-represented	7.65e-6	6.36e-5	14	hsa-miR-122-5p; hsa-miR-125b-5p; hsa-miR-128-3p; hsa-miR-146b-3p; hsa-miR-152-3p; hsa-miR-192-5p; hsa-miR-193a-5p; hsa-miR-193b-5p; hsa-miR-194-5p; hsa-miR-28-3p; hsa-miR-34a-5p; hsa-miR-483-5p; hsa-miR-95-3p; hsa-miR-885-3p
Hypopharynx cancer	over-represented	2.44e-5	1.08e-4	5	hsa-miR-122-5p; hsa-miR-125b-5p; hsa-miR-148a-3p; hsa-miR-27b-3p; hsa-miR-34a-5p
Pancreatic cancer	over-represented	1.63e-5	1.08e-4	18	hsa-miR-122-5p; hsa-miR-125b-5p; hsa-miR-128-3p; hsa-miR-146b-3p; hsa-miR-148a-3p; hsa-miR-152-3p; hsa-miR-192-5p; hsa-miR-193a-5p; hsa-miR-193b-5p; hsa-miR-194-5p; hsa-miR-27b-3p; hsa-miR-28-3p; hsa-miR-30d-5p; hsa-miR-34a-5p; hsa-miR-378c; hsa-miR-483-5p; hsa-miR-95-3p; hsa-miR-885-3p
Nasopharyngeal cancer	over-represented	2.89e-5	1.21e-4	13	hsa-miR-122-5p; hsa-miR-125b-5p; hsa-miR-128-3p; hsa-miR-148a-3p; hsa-miR-152-3p; hsa-miR-193b-5p; hsa-miR-194-5p; hsa-miR-27b-3p; hsa-miR-28-3p; hsa-miR-30d-5p; hsa-miR-34a-5p; hsa-miR-483-5p; hsa-miR-885-3p
Ovarian cancer	over-represented	3.94e-5	1.49e-4	10	hsa-miR-125b-5p; hsa-miR-128-3p; hsa-miR-148a-3p; hsa-miR-152-3p; hsa-miR-192-5p; hsa-miR-194-5p; hsa-miR-27b-3p; hsa-miR-30d-5p; hsa-miR-34a-5p; hsa-miR-483-5p
Colorectal cancer	over-represented	5.59e-5	2.01e-4	17	hsa-miR-122-5p; hsa-miR-125b-5p; hsa-miR-128-3p; hsa-miR-146b-3p; hsa-miR-148a-3p; hsa-miR-152-3p; hsa-miR-192-5p; hsa-miR-193a-5p; hsa-miR-193b-5p; hsa-miR-194-5p; hsa-miR-27b-3p; hsa-miR-28-3p; hsa-miR-30d-5p; hsa-miR-34a-5p; hsa-miR-378c; hsa-miR-483-5p; hsa-miR-95-3p
Head and neck cancer	over-represented	5.59e-5	2.01e-4	8	hsa-miR-122-5p; hsa-miR-125b-5p; hsa-miR-128-3p; hsa-miR-148a-3p; hsa-miR-152-3p; hsa-miR-194-5p; hsa-miR-30d-5p; hsa-miR-95-3p
Small cell lung cancer	over-represented	5.57e-5	2.01e-4	9	hsa-miR-125b-5p; hsa-miR-128-3p; hsa-miR-148a-3p; hsa-miR-152-3p; hsa-miR-193a-5p; hsa-miR-30d-5p; hsa-miR-34a-5p; hsa-miR-483-5p; hsa-miR-95-3p
Urinary bladder cancer	over-represented	2.31e-4	7.62e-4	6	hsa-miR-125b-5p; hsa-miR-152-3p; hsa-miR-193a-5p; hsa-miR-194-5p; hsa-miR-27b-3p; hsa-miR-28-3p

Uterus cancer	over-represented	2.63e-4	8.46e-4	6	hsa-miR-122-5p; hsa-miR-128-3p; hsa-miR-148a-3p; hsa-miR-192-5p; hsa-miR-194-5p; hsa-miR-34a-5p
Germ cell and embryonal cancer	over-represented	4.04e-4	0.0010687	4	hsa-miR-122-5p; hsa-miR-125b-5p; hsa-miR-148a-3p; hsa-miR-34a-5p
Thyroid cancer	over-represented	4.75e-4	0.0011745	7	hsa-miR-125b-5p; hsa-miR-148a-3p; hsa-miR-152-3p; hsa-miR-193b-5p; hsa-miR-27b-3p; hsa-miR-30d-5p; hsa-miR-34a-5p
Kidney cancer	over-represented	5.40e-4	0.0012946	5	hsa-miR-122-5p; hsa-miR-125b-5p; hsa-miR-194-5p; hsa-miR-34a-5p; hsa-miR-483-5p
Tongue cancer	over-represented	5.85e-4	0.0013785	4	hsa-miR-122-5p; hsa-miR-125b-5p; hsa-miR-148a-3p; hsa-miR-34a-5p
Skin cancer	over-represented	6.27e-4	0.0014627	4	hsa-miR-122-5p; hsa-miR-125b-5p; hsa-miR-148a-3p; hsa-miR-34a-5p
Mixed cell type cancer	over-represented	7.71e-4	0.0017306	2	hsa-miR-125b-5p; hsa-miR-34a-5p
Kidney chromophobe cancer	over-represented	7.91e-4	0.0017644	9	hsa-miR-146b-3p; hsa-miR-152-3p; hsa-miR-192-5p; hsa-miR-193a-5p; hsa-miR-193b-5p; hsa-miR-194-5p; hsa-miR-27b-3p; hsa-miR-30d-5p; hsa-miR-95-3p
Sporadic breast cancer	over-represented	0.0010747	0.0023153	2	hsa-miR-125b-5p; hsa-miR-34a-5p
Tonsil cancer	over-represented	0.001137	0.0024344	6	hsa-miR-125b-5p; hsa-miR-128-3p; hsa-miR-192-5p; hsa-miR-30d-5p; hsa-miR-34a-5p; hsa-miR-95-3p
Familial ovarian cancer	over-represented	0.0013877	0.0029087	10	hsa-miR-122-5p; hsa-miR-128-3p; hsa-miR-148a-3p; hsa-miR-152-3p; hsa-miR-192-5p; hsa-miR-193a-5p; hsa-miR-193b-5p; hsa-miR-30d-5p; hsa-miR-483-5p; hsa-miR-95-3p
Gallbladder cancer	over-represented	0.0014267	0.0029549	2	hsa-miR-125b-5p; hsa-miR-34a-5p
Breast cancer her3+ negative	over-represented	0.0017589	0.0035793	10	hsa-miR-122-5p; hsa-miR-125b-5p; hsa-miR-128-3p; hsa-miR-146b-3p; hsa-miR-152-3p; hsa-miR-193a-5p; hsa-miR-193b-5p; hsa-miR-28-3p; hsa-miR-483-5p; hsa-miR-885-3p
Uterine cancer	over-represented	0.0021991	0.0043607	5	hsa-miR-122-5p; hsa-miR-128-3p; hsa-miR-148a-3p; hsa-miR-192-5p; hsa-miR-34a-5p
Ocular cancer	over-represented	0.0033036	0.00637	2	hsa-miR-125b-5p; hsa-miR-34a-5p
Esophageal cancer	over-represented	0.0038809	0.007361	13	hsa-miR-122-5p; hsa-miR-125b-5p; hsa-miR-128-3p; hsa-miR-148a-3p; hsa-miR-152-3p; hsa-miR-192-5p; hsa-miR-193a-5p; hsa-miR-194-5p; hsa-miR-27b-3p; hsa-miR-28-3p; hsa-miR-30d-5p; hsa-miR-95-3p; hsa-miR-885-3p
Adrenal cortex cancer	over-represented	0.004054	0.0076068	3	hsa-miR-125b-5p; hsa-miR-148a-3p; hsa-miR-34a-5p
Testicular cancer	over-represented	0.0051655	0.0091049	3	hsa-miR-122-5p; hsa-miR-125b-5p; hsa-miR-34a-5p
Salivary gland cancer	over-represented	0.0054694	0.0092887	3	hsa-miR-125b-5p; hsa-miR-148a-3p; hsa-miR-34a-5p
Hematologic cancer	over-represented	0.0061093	0.0100573	3	hsa-miR-148a-3p; hsa-miR-152-3p; hsa-miR-34a-5p
Brain cancer	over-represented	0.0091103	0.0134156	3	hsa-miR-125b-5p; hsa-miR-148a-3p; hsa-miR-152-3p

Germ cell cancer	over-represented	0.0101009	0.0147191	2	hsa-miR-125b-5p; hsa-miR-34a-5p
Gastric cancer	over-represented	0.0111548	0.0160537	16	hsa-miR-122-5p; hsa-miR-125b-5p; hsa-miR-146b-3p; hsa-miR-148a-3p; hsa-miR-152-3p; hsa-miR-192-5p; hsa-miR-193a-5p; hsa-miR-193b-5p; hsa-miR-194-5p; hsa-miR-27b-3p; hsa-miR-28-3p; hsa-miR-30d-5p; hsa-miR-34a-5p; hsa-miR-483-5p; hsa-miR-95-3p; hsa-miR-885-3p
Triple negative breast cancer	over-represented	0.0152907	0.0206041	2	hsa-miR-27b-3p; hsa-miR-34a-5p
Endometrial cancer	over-represented	0,0161582	0.0216476	3	hsa-miR-125b-5p; hsa-miR-152-3p; hsa-miR-194-5p
Non-small cell lung cancer	over-represented	0,0186097	0.024695	3	hsa-miR-128-3p; hsa-miR-34a-5p; hsa-miR-483-5p
Colon cancer	over-represented	0.0327542	0.0397608	16	hsa-miR-122-5p; hsa-miR-125b-5p; hsa-miR-128-3p; hsa-miR-146b-3p; hsa-miR-148a-3p; hsa-miR-152-3p; hsa-miR-192-5p; hsa-miR-193a-5p; hsa-miR-194-5p; hsa-miR-27b-3p; hsa-miR-28-3p; hsa-miR-30d-5p; hsa-miR-34a-5p; hsa-miR-378c; hsa-miR-483-5p; hsa-miR-95-3p
Stomach cancer	over-represented	0.0385148	0.0457199	14	hsa-miR-125b-5p; hsa-miR-146b-3p; hsa-miR-148a-3p; hsa-miR-152-3p; hsa-miR-193a-5p; hsa-miR-193b-5p; hsa-miR-194-5p; hsa-miR-27b-3p; hsa-miR-28-3p; hsa-miR-30d-5p; hsa-miR-34a-5p; hsa-miR-483-5p; hsa-miR-95-3p; hsa-miR-885-3p
Module blue					
Breast cancer	over-represented	3.87e-12	1.58e-10	36	hsa-miR-130b-3p; hsa-miR-145-5p; hsa-miR-15b-3p; hsa-miR-15b-5p; hsa-miR-17-5p; hsa-miR-18a-5p; hsa-miR-1908-5p; hsa-miR-195-5p; hsa-miR-204-5p; hsa-miR-205-5p; hsa-miR-222-3p; hsa-miR-30b-5p; hsa-miR-30c-5p; hsa-miR-335-3p; hsa-miR-339-3p; hsa-miR-339-5p; hsa-miR-33a-5p; hsa-miR-345-5p; hsa-miR-421; hsa-miR-425-3p; hsa-miR-450b-5p; hsa-miR-454-5p; hsa-miR-483-3p; hsa-miR-491-5p; hsa-miR-505-5p; hsa-miR-532-3p; hsa-miR-628-5p; hsa-miR-664a-3p; hsa-miR-365a-3p; hsa-miR-548z; hsa-miR-766-3p; hsa-let-7b-3p; hsa-let-7f-2-3p; hsa-miR-1296-5p; hsa-miR-133a-3p; hsa-miR-7-1-3p
Kidney chromophobe cancer	over-represented	4.50e-10	1.11e-8	23	hsa-miR-1306-5p; hsa-miR-130b-3p; hsa-miR-145-5p; hsa-miR-15b-3p; hsa-miR-15b-5p; hsa-miR-18a-5p; hsa-miR-195-5p; hsa-miR-204-5p; hsa-miR-222-3p; hsa-miR-30b-5p; hsa-miR-30c-5p; hsa-miR-335-3p; hsa-miR-425-3p; hsa-miR-450b-5p; hsa-miR-483-3p; hsa-miR-505-5p; hsa-miR-664a-3p; hsa-miR-365a-3p; hsa-miR-365b-3p; hsa-miR-766-3p; hsa-let-7b-3p; hsa-miR-133a-3p; hsa-miR-7-1-3p
Lung cancer	over-represented	5.64e-10	1.30e-8	29	hsa-miR-130b-3p; hsa-miR-145-5p; hsa-miR-15b-5p; hsa-miR-17-5p; hsa-miR-18a-5p; hsa-miR-195-5p; hsa-miR-204-5p; hsa-miR-205-5p; hsa-miR-222-3p; hsa-miR-30b-5p; hsa-miR-30c-5p; hsa-miR-339-3p;

					hsa-miR-339-5p; hsa-miR-33a-5p; hsa-miR-345-5p; hsa-miR-421; hsa-miR-425-3p; hsa-miR-450b-5p; hsa-miR-483-3p; hsa-miR-491-5p; hsa-miR-532-3p; hsa-miR-628-5p; hsa-miR-664a-3p; hsa-miR-365a-3p; hsa-miR-766-3p; hsa-let-7b-3p; hsa-let-7f-2-3p; hsa-miR-1296-5p; hsa-miR-133a-3p
Progesterone-receptor positive breast cancer	over-represented	7.14e-10	1.55e-8	29	hsa-miR-130b-3p; hsa-miR-145-5p; hsa-miR-15b-3p; hsa-miR-15b-5p; hsa-miR-17-5p; hsa-miR-18a-5p; hsa-miR-1908-5p; hsa-miR-195-5p; hsa-miR-204-5p; hsa-miR-205-5p; hsa-miR-222-3p; hsa-miR-30b-5p; hsa-miR-30c-5p; hsa-miR-335-3p; hsa-miR-339-3p; hsa-miR-339-5p; hsa-miR-33a-5p; hsa-miR-345-5p; hsa-miR-421; hsa-miR-425-3p; hsa-miR-454-5p; hsa-miR-483-3p; hsa-miR-505-5p; hsa-miR-532-3p; hsa-miR-664a-3p; hsa-miR-766-3p; hsa-let-7b-3p; hsa-miR-133a-3p; hsa-miR-7-1-3p
Prostate cancer	over-represented	8.36e-10	1.66e-8	27	hsa-miR-130b-3p; hsa-miR-145-5p; hsa-miR-15b-5p; hsa-miR-17-5p; hsa-miR-18a-5p; hsa-miR-195-5p; hsa-miR-204-5p; hsa-miR-205-5p; hsa-miR-222-3p; hsa-miR-30b-5p; hsa-miR-30c-5p; hsa-miR-335-3p; hsa-miR-33a-5p; hsa-miR-345-5p; hsa-miR-421; hsa-miR-425-3p; hsa-miR-450b-5p; hsa-miR-483-3p; hsa-miR-491-5p; hsa-miR-505-5p; hsa-miR-532-3p; hsa-miR-628-5p; hsa-miR-365a-3p; hsa-miR-766-3p; hsa-let-7b-3p; hsa-miR-133a-3p; hsa-miR-7-1-3p
Her2-receptor positive breast cancer	over-represented	1.07e-9	2.06e-8	28	hsa-miR-130b-3p; hsa-miR-145-5p; hsa-miR-15b-3p; hsa-miR-15b-5p; hsa-miR-17-5p; hsa-miR-18a-5p; hsa-miR-1908-5p; hsa-miR-195-5p; hsa-miR-204-5p; hsa-miR-205-5p; hsa-miR-222-3p; hsa-miR-30b-5p; hsa-miR-30c-5p; hsa-miR-335-3p; hsa-miR-339-3p; hsa-miR-339-5p; hsa-miR-33a-5p; hsa-miR-345-5p; hsa-miR-425-3p; hsa-miR-454-5p; hsa-miR-483-3p; hsa-miR-505-5p; hsa-miR-532-3p; hsa-miR-664a-3p; hsa-miR-766-3p; hsa-let-7b-3p; hsa-miR-133a-3p; hsa-miR-7-1-3p
Colorectal cancer	over-represented	1.44e-8	2.08e-7	35	hsa-miR-130b-3p; hsa-miR-145-5p; hsa-miR-15b-5p; hsa-miR-17-5p; hsa-miR-18a-5p; hsa-miR-1908-5p; hsa-miR-195-5p; hsa-miR-204-5p; hsa-miR-205-5p; hsa-miR-222-3p; hsa-miR-30b-5p; hsa-miR-30c-5p; hsa-miR-335-3p; hsa-miR-339-3p; hsa-miR-339-5p; hsa-miR-33a-5p; hsa-miR-345-5p; hsa-miR-3679-5p; hsa-miR-421; hsa-miR-425-3p; hsa-miR-450b-5p; hsa-miR-454-5p; hsa-miR-483-3p; hsa-miR-491-5p; hsa-miR-532-3p; hsa-miR-628-5p; hsa-miR-664a-3p; hsa-miR-365a-3p; hsa-miR-548z; hsa-miR-766-3p; hsa-let-7b-3p; hsa-let-7f-2-3p; hsa-miR-1296-5p; hsa-miR-133a-3p; hsa-miR-7-1-3p

Head and neck cancer	over-represented	2.12e-8	2.94e-7	16	hsa-miR-130b-3p; hsa-miR-145-5p; hsa-miR-17-5p; hsa-miR-18a-5p; hsa-miR-195-5p; hsa-miR-204-5p; hsa-miR-205-5p; hsa-miR-222-3p; hsa-miR-30b-5p; hsa-miR-30c-5p; hsa-miR-339-5p; hsa-miR-33a-5p; hsa-miR-421; hsa-miR-491-5p; hsa-miR-766-3p; hsa-miR-133a-3p
Estrogen-receptor positive breast cancer	over-represented	3.49e-8	4.57e-7	27	hsa-miR-130b-3p; hsa-miR-145-5p; hsa-miR-15b-3p; hsa-miR-15b-5p; hsa-miR-17-5p; hsa-miR-18a-5p; hsa-miR-1908-5p; hsa-miR-195-5p; hsa-miR-204-5p; hsa-miR-205-5p; hsa-miR-222-3p; hsa-miR-30b-5p; hsa-miR-30c-5p; hsa-miR-335-3p; hsa-miR-339-3p; hsa-miR-339-5p; hsa-miR-33a-5p; hsa-miR-345-5p; hsa-miR-421; hsa-miR-425-3p; hsa-miR-454-5p; hsa-miR-483-3p; hsa-miR-505-5p; hsa-miR-532-3p; hsa-miR-766-3p; hsa-let-7b-3p; hsa-miR-7-1-3p
Progesterone-receptor negative breast cancer	over-represented	4.63e-8	5.35e-7	26	hsa-miR-130b-3p; hsa-miR-145-5p; hsa-miR-15b-3p; hsa-miR-15b-5p; hsa-miR-17-5p; hsa-miR-18a-5p; hsa-miR-1908-5p; hsa-miR-195-5p; hsa-miR-204-5p; hsa-miR-205-5p; hsa-miR-222-3p; hsa-miR-30b-5p; hsa-miR-30c-5p; hsa-miR-335-3p; hsa-miR-339-3p; hsa-miR-339-5p; hsa-miR-33a-5p; hsa-miR-421; hsa-miR-425-3p; hsa-miR-454-5p; hsa-miR-483-3p; hsa-miR-664a-3p; hsa-miR-766-3p; hsa-let-7b-3p; hsa-miR-133a-3p; hsa-miR-7-1-3p
Nasopharyngeal cancer	over-represented	7.49e-8	8.11e-7	25	hsa-miR-145-5p; hsa-miR-15b-3p; hsa-miR-15b-5p; hsa-miR-17-5p; hsa-miR-18a-5p; hsa-miR-1908-5p; hsa-miR-195-5p; hsa-miR-204-5p; hsa-miR-205-5p; hsa-miR-222-3p; hsa-miR-30b-5p; hsa-miR-30c-5p; hsa-miR-339-3p; hsa-miR-339-5p; hsa-miR-421; hsa-miR-450b-5p; hsa-miR-454-5p; hsa-miR-483-3p; hsa-miR-491-5p; hsa-miR-505-5p; hsa-miR-532-3p; hsa-miR-628-5p; hsa-miR-365a-3p; hsa-miR-766-3p; hsa-miR-7-1-3p
Estrogen-receptor negative breast cancer	over-represented	1.53e-7	1.55e-6	25	hsa-miR-130b-3p; hsa-miR-145-5p; hsa-miR-15b-3p; hsa-miR-15b-5p; hsa-miR-17-5p; hsa-miR-18a-5p; hsa-miR-1908-5p; hsa-miR-195-5p; hsa-miR-204-5p; hsa-miR-205-5p; hsa-miR-222-3p; hsa-miR-30b-5p; hsa-miR-30c-5p; hsa-miR-335-3p; hsa-miR-339-3p; hsa-miR-339-5p; hsa-miR-33a-5p; hsa-miR-421; hsa-miR-425-3p; hsa-miR-454-5p; hsa-miR-483-3p; hsa-miR-532-3p; hsa-miR-766-3p; hsa-let-7b-3p; hsa-miR-7-1-3p
Small cell lung cancer	over-represented	1.72e-7	1.72e-6	17	hsa-miR-130b-3p; hsa-miR-145-5p; hsa-miR-15b-3p; hsa-miR-15b-5p; hsa-miR-17-5p; hsa-miR-18a-5p; hsa-miR-195-5p; hsa-miR-222-3p; hsa-miR-30b-5p; hsa-miR-30c-5p; hsa-miR-335-3p; hsa-miR-345-5p; hsa-miR-421; hsa-miR-491-5p; hsa-miR-505-5p; hsa-miR-628-5p; hsa-miR-7-1-3p

Thyroid cancer	over-represented	1.90e-7	1.85e-6	15	hsa-miR-145-5p; hsa-miR-15b-3p; hsa-miR-15b-5p; hsa-miR-17-5p; hsa-miR-18a-5p; hsa-miR-195-5p; hsa-miR-204-5p; hsa-miR-205-5p; hsa-miR-222-3p; hsa-miR-335-3p; hsa-miR-339-5p; hsa-miR-345-5p; hsa-miR-421; hsa-miR-133a-3p; hsa-miR-7-1-3p
Bladder cancer	over-represented	2.29e-7	2.17e-6	12	hsa-miR-130b-3p; hsa-miR-145-5p; hsa-miR-17-5p; hsa-miR-18a-5p; hsa-miR-195-5p; hsa-miR-204-5p; hsa-miR-205-5p; hsa-miR-30c-5p; hsa-miR-483-3p; hsa-miR-532-3p; hsa-miR-365a-3p; hsa-miR-133a-3p
Pancreatic cancer	over-represented	9.43e-7	7.78e-6	34	hsa-miR-130b-3p; hsa-miR-145-5p; hsa-miR-15b-3p; hsa-miR-15b-5p; hsa-miR-17-5p; hsa-miR-18a-5p; hsa-miR-1908-5p; hsa-miR-195-5p; hsa-miR-204-5p; hsa-miR-205-5p; hsa-miR-222-3p; hsa-miR-30b-5p; hsa-miR-30c-5p; hsa-miR-335-3p; hsa-miR-339-5p; hsa-miR-33a-5p; hsa-miR-345-5p; hsa-miR-3679-5p; hsa-miR-421; hsa-miR-425-3p; hsa-miR-450b-5p; hsa-miR-454-5p; hsa-miR-483-3p; hsa-miR-491-5p; hsa-miR-505-5p; hsa-miR-532-3p; hsa-miR-628-5p; hsa-miR-664a-3p; hsa-miR-365a-3p; hsa-miR-766-3p; hsa-let-7b-3p; hsa-let-7f-2-3p; hsa-miR-1296-5p; hsa-miR-7-1-3p
Breast cancer luminal	over-represented	1.56e-6	1.21e-5	15	hsa-miR-130b-3p; hsa-miR-145-5p; hsa-miR-15b-5p; hsa-miR-17-5p; hsa-miR-18a-5p; hsa-miR-204-5p; hsa-miR-222-3p; hsa-miR-335-3p; hsa-miR-339-5p; hsa-miR-33a-5p; hsa-miR-345-5p; hsa-miR-421; hsa-miR-483-3p; hsa-let-7b-3p; hsa-miR-7-1-3p
Uterine cancer	over-represented	2.93e-6	2.05e-5	11	hsa-miR-130b-3p; hsa-miR-145-5p; hsa-miR-18a-5p; hsa-miR-195-5p; hsa-miR-204-5p; hsa-miR-205-5p; hsa-miR-222-3p; hsa-miR-339-5p; hsa-miR-33a-5p; hsa-miR-345-5p; hsa-miR-7-1-3p
Testicular germ cell cancer	over-represented	7.85e-6	3.93e-5	10	hsa-miR-130b-3p; hsa-miR-145-5p; hsa-miR-15b-3p; hsa-miR-195-5p; hsa-miR-335-3p; hsa-miR-483-3p; hsa-miR-628-5p; hsa-let-7b-3p; hsa-miR-133a-3p; hsa-miR-7-1-3p
Hypopharynx cancer	over-represented	9.28e-6	4.20e-5	7	hsa-miR-145-5p; hsa-miR-15b-5p; hsa-miR-17-5p; hsa-miR-195-5p; hsa-miR-222-3p; hsa-miR-30b-5p; hsa-miR-133a-3p
Endometrial cancer	over-represented	1.23e-5	5.12e-5	8	hsa-miR-130b-3p; hsa-miR-145-5p; hsa-miR-17-5p; hsa-miR-18a-5p; hsa-miR-195-5p; hsa-miR-205-5p; hsa-miR-222-3p; hsa-miR-30c-5p
Ovarian cancer	over-represented	1.63e-5	6.39e-5	16	hsa-miR-130b-3p; hsa-miR-17-5p; hsa-miR-18a-5p; hsa-miR-1908-5p; hsa-miR-205-5p; hsa-miR-30b-5p; hsa-miR-30c-5p; hsa-miR-339-3p; hsa-miR-339-5p; hsa-miR-33a-5p; hsa-miR-345-5p; hsa-miR-421; hsa-miR-483-3p; hsa-miR-532-3p; hsa-miR-664a-3p; hsa-miR-766-3p

Skin cancer	over-represented	1.76e-5	6.69e-5	7	hsa-miR-145-5p; hsa-miR-17-5p; hsa-miR-18a-5p; hsa-miR-195-5p; hsa-miR-205-5p; hsa-miR-222-3p; hsa-miR-133a-3p
Urinary bladder cancer	over-represented	1.75e-5	6.69e-5	10	hsa-miR-130b-3p; hsa-miR-145-5p; hsa-miR-15b-5p; hsa-miR-195-5p; hsa-miR-204-5p; hsa-miR-222-3p; hsa-miR-30b-5p; hsa-miR-483-3p; hsa-miR-532-3p; hsa-miR-365a-3p
Non-small cell lung cancer	over-represented	1.82e-5	6.91e-5	8	hsa-miR-130b-3p; hsa-miR-145-5p; hsa-miR-17-5p; hsa-miR-18a-5p; hsa-miR-205-5p; hsa-miR-222-3p; hsa-miR-30b-5p; hsa-miR-30c-5p
Uterus cancer	over-represented	2.15e-5	8.02e-5	10	hsa-miR-130b-3p; hsa-miR-145-5p; hsa-miR-18a-5p; hsa-miR-195-5p; hsa-miR-204-5p; hsa-miR-205-5p; hsa-miR-222-3p; hsa-miR-339-5p; hsa-miR-33a-5p; hsa-miR-345-5p
Breast cancer her3+ negative	over-represented	2.44e-5	8.92e-5	20	hsa-miR-130b-3p; hsa-miR-145-5p; hsa-miR-15b-3p; hsa-miR-15b-5p; hsa-miR-17-5p; hsa-miR-18a-5p; hsa-miR-1908-5p; hsa-miR-195-5p; hsa-miR-204-5p; hsa-miR-205-5p; hsa-miR-222-3p; hsa-miR-30c-5p; hsa-miR-335-3p; hsa-miR-339-3p; hsa-miR-339-5p; hsa-miR-425-3p; hsa-miR-454-5p; hsa-miR-483-3p; hsa-miR-766-3p; hsa-let-7b-3p
Adrenal cortex cancer	over-represented	5.17e-5	1.80e-4	6	hsa-miR-145-5p; hsa-miR-17-5p; hsa-miR-18a-5p; hsa-miR-195-5p; hsa-miR-205-5p; hsa-miR-222-3p
Familial ovarian cancer	over-represented	6.32e-5	2.15e-4	19	hsa-miR-15b-3p; hsa-miR-15b-5p; hsa-miR-17-5p; hsa-miR-18a-5p; hsa-miR-195-5p; hsa-miR-30c-5p; hsa-miR-335-3p; hsa-miR-339-3p; hsa-miR-339-5p; hsa-miR-33a-5p; hsa-miR-421; hsa-miR-425-3p; hsa-miR-454-5p; hsa-miR-491-5p; hsa-miR-505-5p; hsa-miR-532-3p; hsa-miR-628-5p; hsa-let-7b-3p; hsa-miR-7-1-3p
Germ cell and embryonal cancer	over-represented	9.52e-5	2.51e-4	6	hsa-miR-145-5p; hsa-miR-15b-5p; hsa-miR-17-5p; hsa-miR-222-3p; hsa-miR-30b-5p; hsa-miR-133a-3p
Salivary gland cancer	over-represented	9.52e-5	2.51e-4	6	hsa-miR-145-5p; hsa-miR-17-5p; hsa-miR-18a-5p; hsa-miR-195-5p; hsa-miR-205-5p; hsa-miR-222-3p
Gastric cancer	over-represented	1.22e-4	2.97e-4	34	hsa-miR-1306-5p; hsa-miR-130b-3p; hsa-miR-145-5p; hsa-miR-15b-3p; hsa-miR-15b-5p; hsa-miR-17-5p; hsa-miR-18a-5p; hsa-miR-1908-5p; hsa-miR-195-5p; hsa-miR-204-5p; hsa-miR-205-5p; hsa-miR-222-3p; hsa-miR-30b-5p; hsa-miR-30c-5p; hsa-miR-335-3p; hsa-miR-339-5p; hsa-miR-33a-5p; hsa-miR-345-5p; hsa-miR-3679-5p; hsa-miR-421; hsa-miR-425-3p; hsa-miR-450b-5p; hsa-miR-454-5p; hsa-miR-483-3p; hsa-miR-491-5p; hsa-miR-505-5p; hsa-miR-532-3p; hsa-miR-365a-3p; hsa-miR-548z; hsa-miR-766-3p; hsa-let-7b-3p; hsa-let-7f-2-3p; hsa-miR-1296-5p; hsa-miR-133a-3p

Large cell neuroendocrine cancer	over-represented	1.30e-4	3.16e-4	9	hsa-miR-130b-3p; hsa-miR-145-5p; hsa-miR-17-5p; hsa-miR-18a-5p; hsa-miR-195-5p; hsa-miR-30b-5p; hsa-miR-30c-5p; hsa-miR-421; hsa-miR-7-1-3p
Esophageal cancer	over-represented	1.54e-4	3.64e-4	26	hsa-miR-1306-5p; hsa-miR-130b-3p; hsa-miR-145-5p; hsa-miR-15b-3p; hsa-miR-15b-5p; hsa-miR-17-5p; hsa-miR-18a-5p; hsa-miR-1908-5p; hsa-miR-195-5p; hsa-miR-204-5p; hsa-miR-205-5p; hsa-miR-222-3p; hsa-miR-30b-5p; hsa-miR-30c-5p; hsa-miR-335-3p; hsa-miR-339-5p; hsa-miR-33a-5p; hsa-miR-3679-5p; hsa-miR-425-3p; hsa-miR-483-3p; hsa-miR-505-5p; hsa-miR-532-3p; hsa-miR-365a-3p; hsa-miR-766-3p; hsa-let-7b-3p; hsa-miR-133a-3p
Tongue cancer	over-represented	1.64e-4	3.81e-4	6	hsa-miR-145-5p; hsa-miR-17-5p; hsa-miR-18a-5p; hsa-miR-205-5p; hsa-miR-222-3p; hsa-miR-133a-3p
Basal-like breast cancer	over-represented	6.15e-4	0.0012497	10	hsa-miR-130b-3p; hsa-miR-145-5p; hsa-miR-15b-5p; hsa-miR-17-5p; hsa-miR-18a-5p; hsa-miR-195-5p; hsa-miR-33a-5p; hsa-miR-483-3p; hsa-miR-532-3p; hsa-miR-365a-3p
Testicular cancer	over-represented	8.34e-4	0.0016055	5	hsa-miR-145-5p; hsa-miR-17-5p; hsa-miR-18a-5p; hsa-miR-222-3p; hsa-miR-133a-3p
Colon cancer	over-represented	0.0012088	0.002148	34	hsa-miR-1306-5p; hsa-miR-130b-3p; hsa-miR-145-5p; hsa-miR-15b-3p; hsa-miR-15b-5p; hsa-miR-17-5p; hsa-miR-18a-5p; hsa-miR-1908-5p; hsa-miR-195-5p; hsa-miR-204-5p; hsa-miR-205-5p; hsa-miR-222-3p; hsa-miR-30b-5p; hsa-miR-30c-5p; hsa-miR-335-3p; hsa-miR-339-5p; hsa-miR-33a-5p; hsa-miR-345-5p; hsa-miR-3679-5p; hsa-miR-421; hsa-miR-425-3p; hsa-miR-450b-5p; hsa-miR-454-5p; hsa-miR-483-3p; hsa-miR-491-5p; hsa-miR-505-5p; hsa-miR-532-3p; hsa-miR-365a-3p; hsa-miR-766-3p; hsa-let-7b-3p; hsa-let-7f-2-3p; hsa-miR-1296-5p; hsa-miR-133a-3p; hsa-miR-7-1-3p
Rectum cancer	over-represented	0.0014202	0.002498	5	hsa-miR-17-5p; hsa-miR-18a-5p; hsa-miR-195-5p; hsa-miR-205-5p; hsa-miR-222-3p
Brain cancer	over-represented	0.0021054	0.0036359	5	hsa-miR-145-5p; hsa-miR-17-5p; hsa-miR-18a-5p; hsa-miR-195-5p; hsa-miR-205-5p
Cervical cancer	over-represented	0.0025841	0.0043891	4	hsa-miR-145-5p; hsa-miR-17-5p; hsa-miR-205-5p; hsa-miR-491-5p
Kidney cancer	over-represented	0.0034418	0.0056655	6	hsa-miR-145-5p; hsa-miR-17-5p; hsa-miR-18a-5p; hsa-miR-195-5p; hsa-miR-204-5p; hsa-miR-222-3p
Gastrointestinal system cancer	over-represented	0.0052203	0.0083548	4	hsa-miR-145-5p; hsa-miR-17-5p; hsa-miR-18a-5p; hsa-miR-205-5p
Triple negative breast cancer	over-represented	0.0071879	0.0108761	3	hsa-miR-18a-5p; hsa-miR-195-5p; hsa-miR-205-5p
Adrenocortical cancer	over-represented	0.0099642	0.0146608	5	hsa-miR-15b-5p; hsa-miR-195-5p; hsa-miR-33a-5p; hsa-miR-483-3p; hsa-miR-766-3p
Ocular cancer	over-represented	0.0142656	0.0205105	2	hsa-miR-17-5p; hsa-miR-222-3p

Tonsil cancer	over-represented	0.015947	0.0212524	7	hsa-miR-17-5p; hsa-miR-18a-5p; hsa-miR-204-5p; hsa-miR-30b-5p; hsa-miR-30c-5p; hsa-miR-339-5p; hsa-miR-483-3p
Cancer	over-represented	0.0251214	0.0331602	23	hsa-miR-145-5p; hsa-miR-15b-3p; hsa-miR-204-5p; hsa-miR-30c-5p; hsa-miR-335-3p; hsa-miR-339-3p; hsa-miR-33a-5p; hsa-miR-345-5p; hsa-miR-421; hsa-miR-425-3p; hsa-miR-450b-5p; hsa-miR-454-5p; hsa-miR-483-3p; hsa-miR-491-5p; hsa-miR-505-5p; hsa-miR-532-3p; hsa-miR-628-5p; hsa-miR-664a-3p; hsa-miR-365a-3p; hsa-miR-548z; hsa-let-7b-3p; hsa-let-7f-2-3p; hsa-miR-7-1-3p
Small intestine cancer	over-represented	0.0284111	0.0373603	3	hsa-miR-17-5p; hsa-miR-18a-5p; hsa-miR-664a-3p
Ovarian epithelial cancer	over-represented	0.0338419	0.0425634	3	hsa-miR-130b-3p; hsa-miR-145-5p; hsa-miR-205-5p

Supplementary Table 7. Physical activity-associated miRNA gene chromosome locus.

Mirbase id	Chromosome name	Start position	End position
Glaucous			
hsa-mir-1277	X	118386394	118386471
hsa-mir-1307	10	103394253	103394401
hsa-mir-301a	17	59151136	59151221
hsa-mir-30d	8	134804876	134804945
hsa-mir-374a	X	74287286	74287357
hsa-mir-590	7	74191198	74191294
Green			
hsa-mir-122	18	58451074	58451158
hsa-mir-148a	7	25949919	25949986
hsa-mir-152	17	48037161	48037247
hsa-mir-192	11	64891137	64891246
hsa-mir-193a	17	31559996	31560083
hsa-mir-193b	16	14303967	14304049
hsa-mir-27b	9	95085445	95085541
hsa-mir-28	3	188688781	188688866
hsa-mir-3065	17	81125877	81125955
hsa-mir-30d	8	134804876	134804945
hsa-mir-34a	1	9151668	9151777
hsa-mir-378c	10	130962588	130962668
hsa-mir-483	11	2134134	2134209
hsa-mir-885	3	10394489	10394562
hsa-mir-95	4	8005301	8005381
Blue			
hsa-let-7b	22	46113686	46113768
hsa-let-7f-2	X	53557192	53557274
hsa-mir-1296	10	63372957	63373048
hsa-mir-1306	22	20086058	20086142
hsa-mir-130b	22	21653304	21653385
hsa-mir-145	5	149430646	149430733
hsa-mir-15b	3	160404588	160404685
hsa-mir-17	13	91350605	91350688

hsa-mir-18a	13	91350751	91350821
hsa-mir-1908	11	61815161	61815240
hsa-mir-195	17	7017615	7017701
hsa-mir-204	9	70809975	70810084
hsa-mir-205	1	209432133	209432242
hsa-mir-222	X	45747015	45747124
hsa-mir-30b	8	134800520	134800607
hsa-mir-335	7	130496111	130496204
hsa-mir-339	7	1022933	1023026
hsa-mir-33a	22	41900944	41901012
hsa-mir-345	14	100307859	100307956
hsa-mir-365a	16	14309285	14309371
hsa-mir-365b	17	31575411	31575521
hsa-mir-3679	2	134127125	134127192
hsa-mir-421	X	74218377	74218461
hsa-mir-425	3	49020148	49020234
hsa-mir-450b	X	134540185	134540262
hsa-mir-454	17	59137758	59137872
hsa-mir-483	11	2134134	2134209
hsa-mir-491	9	20716105	20716188
hsa-mir-505	X	139924148	139924231
hsa-mir-532	X	50003148	50003238
hsa-mir-548z	12	64622509	64622605
hsa-mir-628	15	55372940	55373034
hsa-mir-664a	1	220200538	220200619
hsa-mir-7-1	9	83969748	83969857
hsa-mir-766	HG2541_PATCH	97740	97850
hsa-mir-766	X	119646738	119646848

3. Supplementary Figures

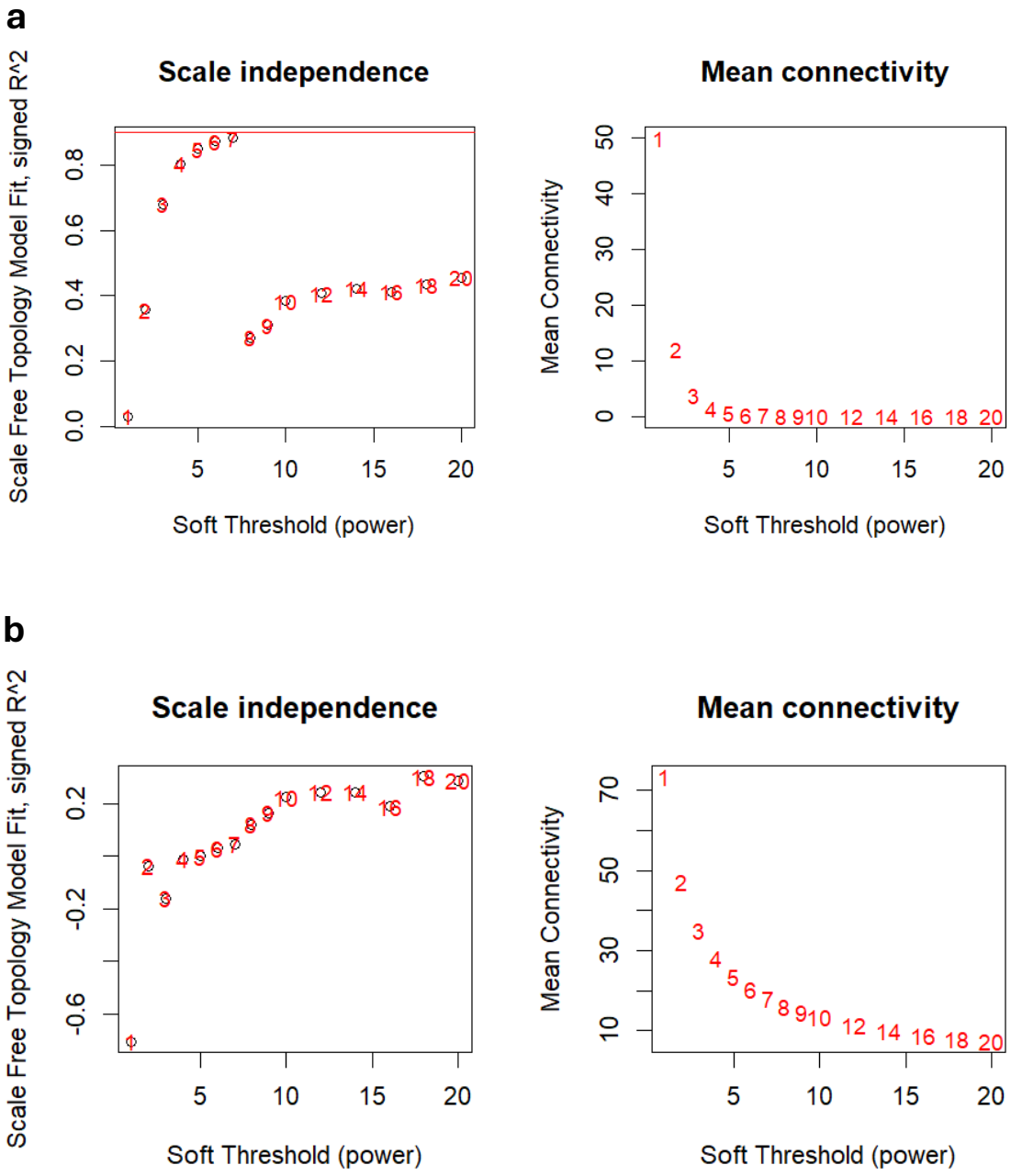

Supplementary Fig. 1. Selection of soft-thresholding power for weighted gene co-expression network analysis (WGCNA) for a) circulating microRNAs and b) circulating metabolites. The left panel shows the scale-free topology model fit (signed R^2) as a function of the soft-thresholding power. A threshold of $R^2 > 0.9$ (red horizontal line) indicates approximate scale-free topology. The right panel displays mean connectivity (average degree) for each power.

a

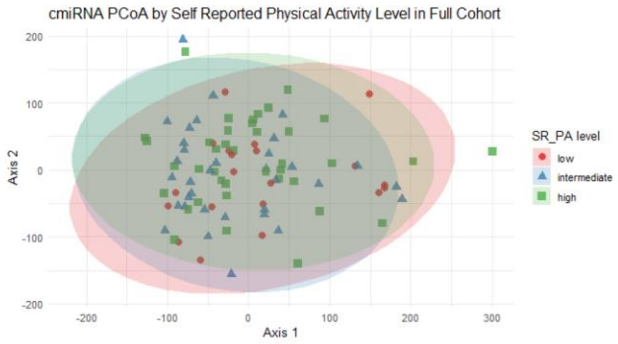

Difference in the full cohort groups' PCoA distance matrix		
SR-PA	PERMANOVA	ANOSIM
low-intermediate-high	*p = 0.390*	*p = 0.217*
low-intermediate	*p = 0.324*	*p = 0.212*
low-high	*p= 0.501*	*p = 0.232*
intermediate-high	*p = 0.315*	*p = 0.432*

b

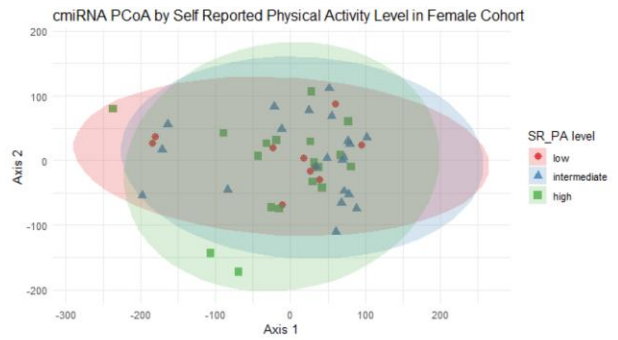

Difference in the female groups' PCoA distance matrix		
SR-PA	PERMANOVA	ANOSIM
low-intermediate-high	*p = 0.502*	*p = 0.470*
low-intermediate	*p = 0.382*	*p = 0.491*
low-high	*p= 0.790*	*p = 0.638*
intermediate-high	*p = 0.327*	*p = 0.326*

c

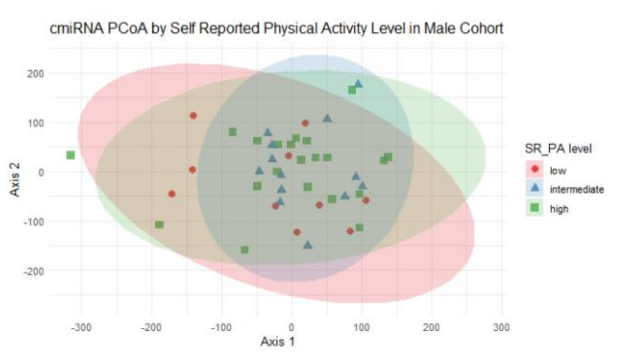

Difference in the male groups' PCoA distance matrix		
SR-PA	PERMANOVA	ANONIM
low-intermediate-high	*p = 0.744*	*p = 0.279*
low-intermediate	*p = 0.443*	*p = 0.148*
low-high	*p= 0.694*	*p = 0.154*
intermediate-high	*p = 0.747*	*p = 0.715*

Supplementary Fig. 2. Differences in circulating microRNA profiles between self-reported physical activity (SR-PA) groups. Principal coordinates analysis (PCoA) was used to study and visualize differences in microRNA expression among participants categorized into low, intermediate, and high physical activity groups in a) full, b) female and c) male cohort. Group differences were statistically assessed using PERMANOVA which tests whether the centroids of groups are significantly different in multivariate space, and ANOSIM, which compares within-group vs between-group distances to see if samples are more similar within groups than between them.

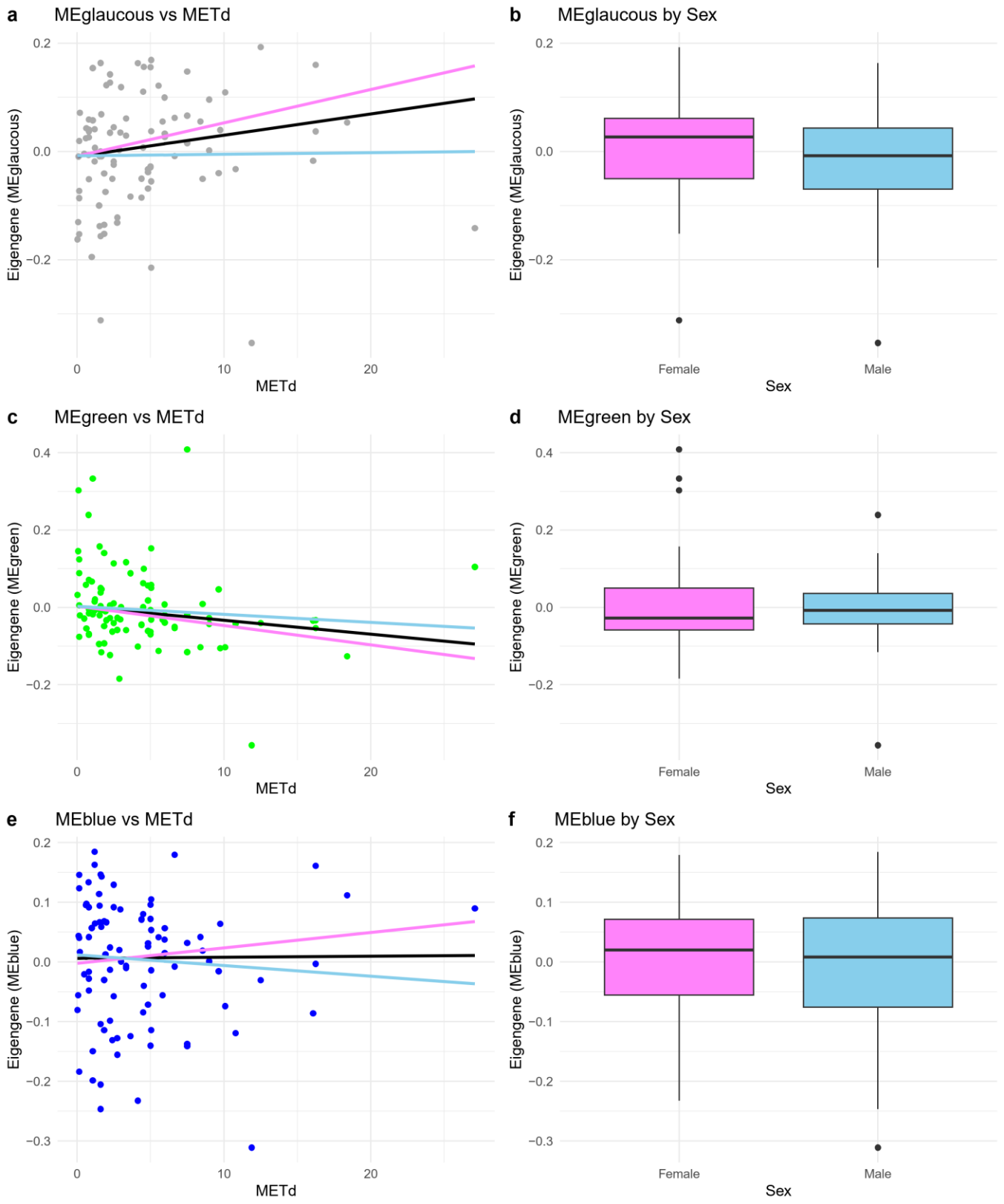

Supplementary Fig. 3. Associations between physical activity and circulating microRNA module eigengenes (ME), stratified by sex. Scatter plots (left) and boxplots (right) illustrate the distribution of module eigengenes (MEglaucous, MEgreen, and MEblue) in relation to daily metabolic equivalents (METd) and sex. Robust linear regression lines are overlaid on the scatter plots to visualize trends across all participants (black), females (pink), and males (blue). Panels a–f show results for MEglaucous, MEgreen, and MEblue, respectively. Boxplots display module eigengene distributions by sex. These plots highlight potential sex-specific trends in the relationship between physical activity and microRNA module expression.

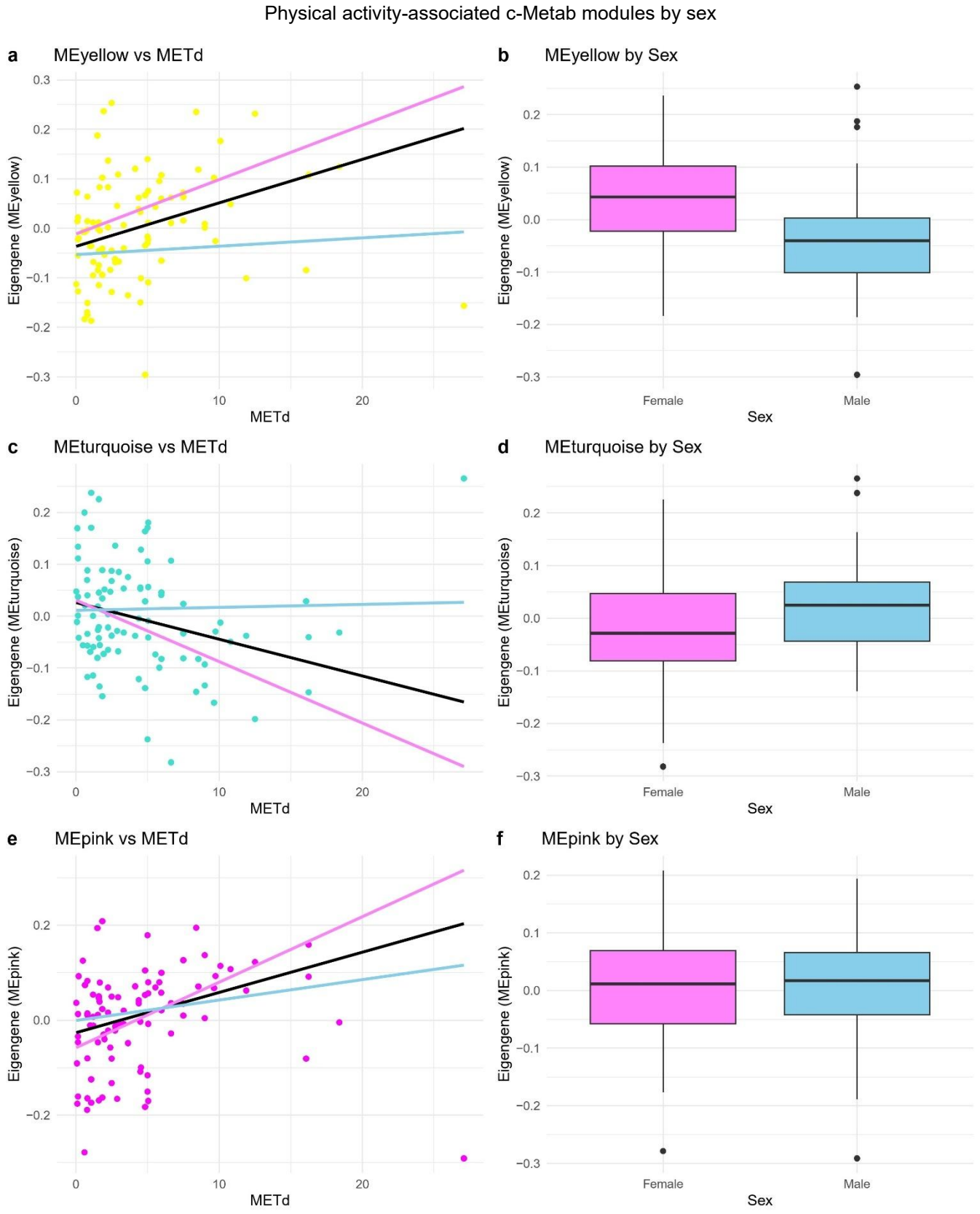

Supplementary Fig. 4. Associations between physical activity and circulating metabolite module eigengenes (ME), stratified by sex. Scatter plots (left) and boxplots (right) illustrate the distribution of module eigengenes (MEyellow, MEturquoise, and MEpink) in relation to daily metabolic equivalents (METd) and sex. Robust linear regression lines are overlaid on the scatter plots to visualize trends across all participants (black), females (pink), and males (blue). Panels a–f show results for MEyellow, MEturquoise, and MEpink, respectively. Boxplots display module eigengene distributions by sex. These plots highlight potential sex-specific trends in the relationship between physical activity and metabolite module levels.

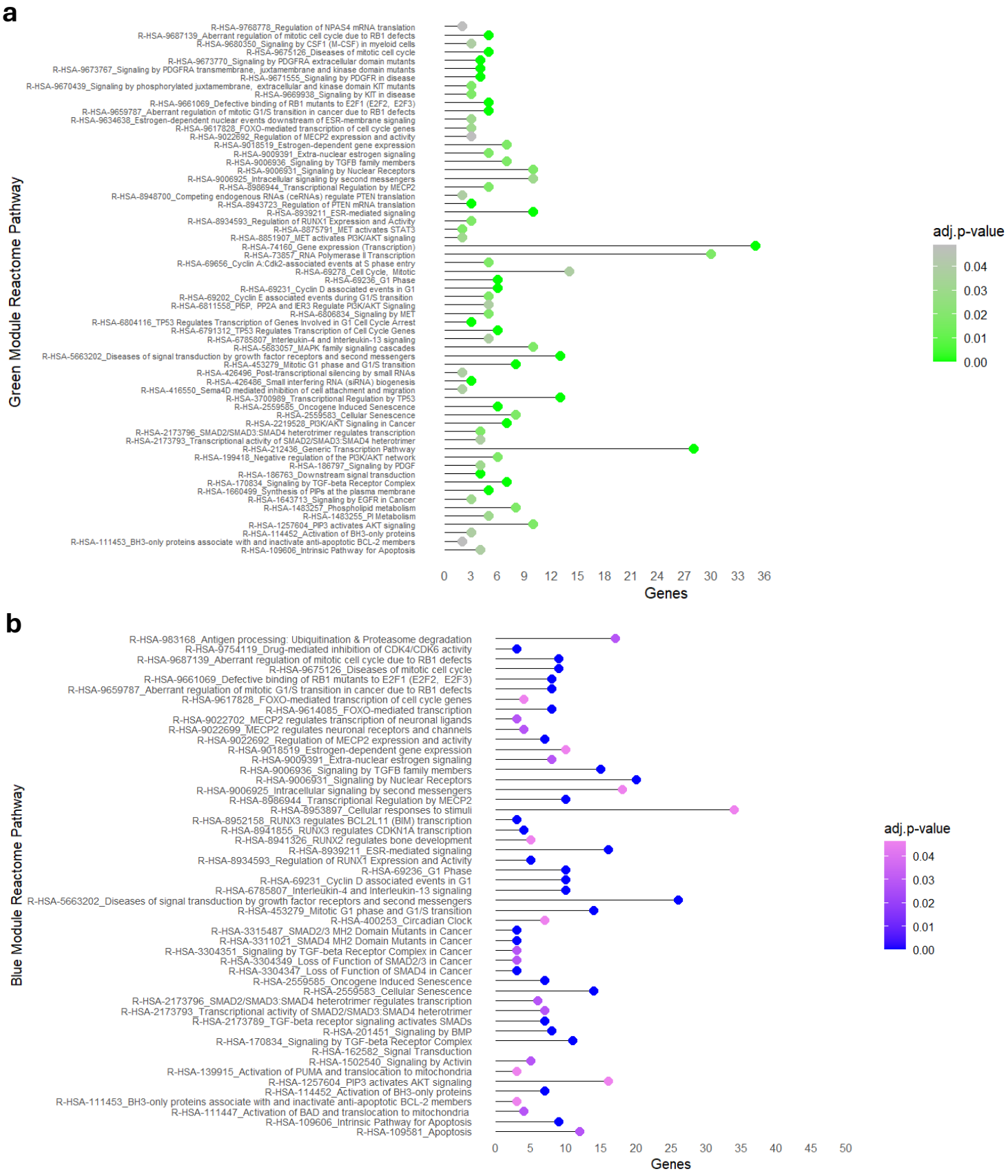

Supplementary Fig. 5. Reactome pathway enrichment of microRNAs in the a) Green and b) Blue modules. Dot plot shows the top enriched Reactome pathways associated with the co-expression modules green and blue. The x-axis represents the number of genes within each pathway, and pathways are listed along the y-axis by Reactome ID and name. Dot color reflects the adjusted p-value (Benjamini–Hochberg correction), with darker blue indicating higher statistical significance. Pathways are related to transcriptional regulation, signal transduction, cell cycle control, and apoptosis.